

Collapse of the charge-ordering state at high magnetic fields in the rare-earth manganite $\text{Pr}_{0.63}\text{Ca}_{0.37}\text{MnO}_3$

K. S. Nagapriya,* A. K. Raychaudhuri,† Bhavtosh Bansal, and V. Venkataraman
Department of Physics, Indian Institute of Science, Bangalore 560 012, India

Sachin Parashar and C. N. R. Rao
Jawaharlal Nehru Center for Advanced Scientific Research, Bangalore, India

We have investigated the specific heat and resistivity of a single crystal of $\text{Pr}_{0.63}\text{Ca}_{0.37}\text{MnO}_3$ around the charge ordering (CO) transition temperature, T_{CO} , in the presence of high magnetic fields (≤ 12 T) which can melt the charge-ordered state. At low magnetic fields (≤ 10 T), the manganite transforms from a charge-disordered paramagnetic insulating (PI) state to a charge-ordered insulating (COI) state as the temperature is lowered. The COI state becomes unstable beyond a threshold magnetic field and melts to a ferromagnetic metallic phase (FMM). This occurs for $T < T_{CO}$. However, above a critical field $\mu_0 H^*$, the sample shows the onset of a metallic phase for $T > T_{CO}$ and the COI transition occurs from a metallic phase. The onset temperature of the high-field metallic behavior decreases with an increase in the field and above a field $\mu_0 H^*$, the COI transition does not occur and the CO state ceases to occur at all T . The entropy change involved in the CO transition, $\Delta S_{CO} \approx 1.6$ J/mol K at 0 T, decreases with increasing field and eventually vanishes for a field $\mu_0 H^*$. The collapse of the CO state above $\mu_0 H^*$ is thus associated with a collapse of the entropy that stabilizes the CO state.

PACS number(s): 75.47.Lx, 64.60.-i

I. INTRODUCTION

Thermodynamic and transport properties of rare-earth manganites with the general formula $R_{1-x}A_x\text{MnO}_3$ (R : a trivalent rare-earth ion; A : a divalent alkaline-earth ion) have attracted considerable current interest.^{1,2} For certain values of x , the Mn^{3+} and Mn^{4+} order in the lattice giving rise to what is called charge ordering. The CO insulating (COI) state can be destabilized by various perturbations such as temperature, magnetic field, electric field and radiation to a ferromagnetic metallic (FMM) or a charge-disordered and paramagnetic insulating (PI) state^{3-8,18}.

Of interest to us is the observation that an applied magnetic field can destabilize the charge-ordered state leading to a ferromagnetic metallic state. This phenomenon has been studied in detail by using various techniques.⁷⁻¹¹ It appears that there is a minimum threshold field $\mu_0 H_{th}$ which is needed to melt the CO state to a FMM phase below T_{CO} . $\mu_0 H_{th}$ depends on a number of factors like the radius of the A site cation, $\langle r_A \rangle$ (equivalently the bandwidth), and deviation from the $x=0.5$ composition which has an equal amount of carriers and holes. $\mu_0 H_{th}$ decreases as $\langle r_A \rangle$ increases and as we move away from the $x=0.5$ filling.² In our present investigation we explore whether there is an upper field $\mu_0 H^*$ ($\mu_0 H^* > \mu_0 H_{th}$) beyond which the CO transition cannot occur at any temperature (i.e., the temperature T_{CO} ceases to exist). We then investigate the region of phase diagram close to $\mu_0 H^*$ and beyond. We note that on comparison of various data available in different CO systems it appears that there is a likelihood of such an upper field as $\mu_0 H^*$.⁸⁻¹¹ The present investigation goes beyond these likely evidences and establishes concretely the existence of such a field.

The cartoon in Fig. 1 explains the issues that we are prob-

ing in this investigation. The cartoon is representative of the currently accepted $(T-\mu_0 H)$ plane phase diagram seen in manganites such as $\text{Pr}_{1-x}\text{Ca}_x\text{MnO}_3$, showing the onset of CO transition from a paramagnetic insulating (PI) that is charge-disordered state. The CO transition occurs at zero field at the temperature T_{CO} , marked by point A. On the application of a magnetic field, T_{CO} generally decreases and follows the line AB. Thus PI \rightarrow COI transition occurs when the line AB is crossed. However, for $\mu_0 H > \mu_0 H_{th}$, the COI state melts to FMM state at $T < T_{CO}$, as mentioned before. The melting of the COI state to the FMM state occurs along the line BC which also shows hysteresis and often strong time dependent

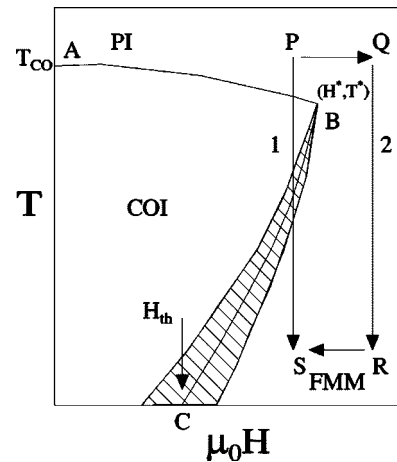


FIG. 1. A cartoon of the $T-\mu_0 H$ plane phase diagram seen in most manganites like $\text{Pr}_{1-x}\text{Ca}_x\text{MnO}_3$ which show the onset of CO transition from a PI (charge disordered) state. COI is charge-ordered insulator and FMM is ferromagnetic metal.

behavior.¹² The low temperature COI \rightarrow FMM transition occurs on crossing line BC. The region bounded by ABC is a region of “mixed phase” where two phases can coexist. The transition across the line AB has a clear thermodynamic signature and is associated with a change in entropy.¹³ In the case of $\text{Pr}_{0.63}\text{Ca}_{0.37}\text{MnO}_3$ ($T_{CO} \approx 235$ K), the entropy removed at T_{CO} at zero magnetic field is ≈ 1.6 J/mol K as found from direct measurements of specific heat.¹³ A good part of the entropy change is released as latent heat and the transition is believed to be of first order. There is no large thermodynamic signature to the transition across the line CB when the COI melts in a magnetic field, although the existence of hysteresis (marked by hatches) as well as the suddenness of the transition is often interpreted as a first order transition. Whatever be the case, there is very little change in the specific heat as well as entropy across the line BC. The field $\mu_0 H^*$ refers to the point B where the two lines meet at temperature T^* . The above phase diagram though known and well established is presented here to put this investigation in proper perspective.

The present investigation is primarily focused on the region around the point B ($\mu_0 H^*, T^*$). The primary motivation is to explore the following issues.

(1) The ($\mu_0 H$ - T) phase diagram as depicted in Fig. 1 is expected to have more features. This can be illustrated as follows. If we cool down following path 1, we start from a PI phase at point P, cross the boundaries AB and BC and terminate in a FMM phase at point S. But if we follow the path 2 (PQRS), we can go from P (PI phase) to S (FMM phase) without any phase transition or crossover region. This implies that somewhere along path 2 there should be a boundary demarcating two phases or a crossover. This should occur for $\mu_0 H > \mu_0 H^*$. We note that this issue has not been raised in previous publications in this field in the context of $\text{Pr}_{0.63}\text{Ca}_{0.37}\text{MnO}_3$, although the phase diagram in this field region where the CO transition ceases to exist has been discussed in a related though different system $\text{Pr}_{0.75}\text{Na}_{0.25}\text{MnO}_3$ which we will discuss in appropriate place.

(2) Our previous studies of specific heat at $\mu_0 H = 0$ and $\mu_0 H = 8$ T have shown that in the transition across the line AB, there is a finite entropy change ($\Delta S_{CO} \neq 0$).¹³ However, there is a negligible change in entropy as one crosses the line CB. One would therefore expect that the nature of the transition changes as one goes along the line AB. We explore the evolution of ΔS_{CO} as we approach the point B. Does $\Delta S_{CO} \rightarrow 0$ as the point B is approached?

(3) At fields lower than $\mu_0 H^*$, the high temperature PI phase makes a transition to the COI phase at T_{CO} which eventually melts at an even lower temperature in a magnetic field, giving rise to the FMM phase. Is there a change associated with the PI phase in a high enough magnetic field? This particular aspect has also not been explicitly discussed or observed before although certain past studies show likely signs of such metallic phases.⁷

We investigate the above issues in a single crystal of $\text{Pr}_{0.63}\text{Ca}_{0.37}\text{MnO}_3$ by using both thermodynamic (specific heat) and transport measurements in a magnetic field up to 12 T. The results of the investigation (discussed in detail in subsequent sections) establish the following.

(1) As we move along the line AB, as $T \rightarrow T^*$ and $\mu_0 H$

$\rightarrow \mu_0 H^*$, $\Delta S_{CO} \rightarrow 0$. Beyond this field, CO does not exist at any temperature. The T_{CO} itself decreases as H increases. The fact that no CO transition takes place when $\Delta S \rightarrow 0$ means that there is an essential role of entropy in stabilizing the CO state.

(2) In the temperature range [$260 \text{ K} > T > T_{CO}(H)$], the PI phase crosses over to a metallic phase for a certain magnetic field. We designate this regime as a metallic regime (M). In this field and temperature regime, the CO transition occurs from a metallic phase, instead of an insulating phase. This gives us a new line of crossover in the (T - $\mu_0 H$) phase diagram. Above 260 K the resistivity reaches a rather field insensitive region.

(3) For fields $\mu_0 H > \mu_0 H^*$ (which is the limit of stability of CO transition) there appears to be the presence of a crossover region (or phase transition) within the metallic phase as it is cooled where long range ferromagnetic order sets in (FMM) at $T \approx 220$ K.

To our knowledge, the studies reported by us are new and they make the qualitative phase diagram in Fig. 1 richer and more complete, particularly in the high field region.

II. EXPERIMENTAL TECHNIQUES

A. Sample

The sample we have chosen for the present investigation $\text{Pr}_{0.63}\text{Ca}_{0.37}\text{MnO}_3$ is a well characterized single crystal, with a well-defined CO transition at $T_{CO} \approx 235$ K. The crystal has been grown by float-zone technique using a mirrorfurnace. This material has been extensively investigated by us. Previously reported¹³ specific heat measurements on this sample from our group showed that the CO transition was most likely first order in nature and the entropy change involved in the transition had been calculated. We note that in the past investigation from our group¹³ the measurements were not done to high enough magnetic field so that one can reach the region (T^*, H^*) and beyond. As a result observations made in the present paper could not be made. In particular we could not observe $\Delta S \rightarrow 0$. Also no concrete connection to transport studies at high fields had been established.

B. Measurement of specific heat in magnetic field

The specific heat was measured using the technique of continuous cooling calorimetry.¹⁴ This is distinct from our studies in Ref. 13 where data were taken by adiabatic calorimetry. The temperature range in which the calorimeter operates is from 100–400 K (this is the temperature range in which the transitions occur). The specific heat in this temperature region was measured in a field up to 10 T. The calorimeter can measure heat capacity of very small samples (mass \sim mg). The addenda heat capacity is < 20 mJ/K at room temperature.

In this method, the sample temperature is recorded as a function of time as the sample (warmed up to a predetermined temperature by a heater) cools continuously, losing heat to the base through a heat link whose characteristics are experimentally determined. The cooling curve is determined by the equation

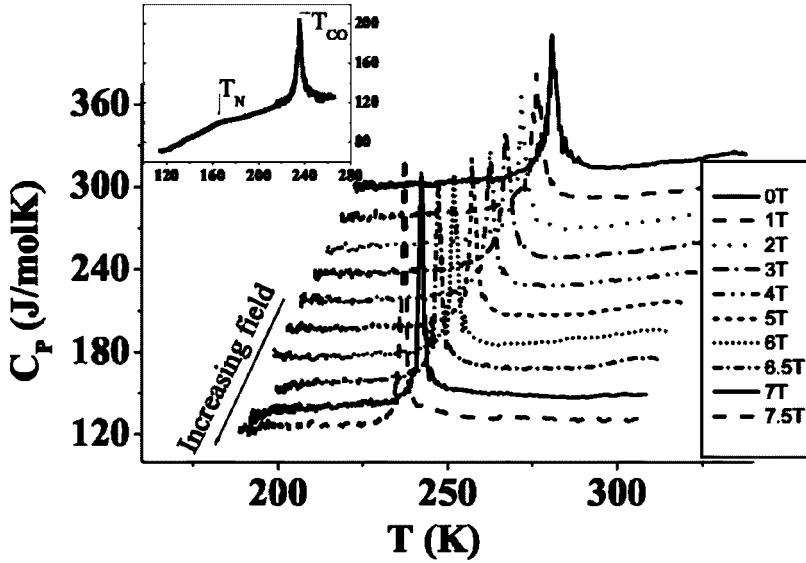


FIG. 2. Waterfall plot of specific heat as a function of temperature at various magnetic fields. Note that the data are offset for clarity. Inset: Specific heat as a function of temperature for zero field over an extended temperature range. Note the T_{CO} at ≈ 235 K and T_N at ≈ 165 K.

$$C(T) \frac{dT}{dt}(T) = -P_{leak}(T), \quad (1)$$

where $P_{leak}(T)$ is the power leaked to the bath [$P_{leak}(T)$ is experimentally determined and has both the conduction and radiation contributions]. A platinum film on the substrate works as both a heater and thermometer. The specific heat and latent heat at a transition are deduced from the cooling curve—by determining $dT/dt(T)$ and the thermal link characteristics. The data obtained by this method matches with that obtained by Ref. 13 which was taken by adiabatic calorimetry which acquires data during heating. There are some differences in the transition region that we discuss. This difference shows up in the transition region as a small change in the width of the transition as well as height of the heat capacity peak. This of course depends on the rate at which temperature changes in this region. However, this does not have much effect when we integrate the excess heat capacity at transition to find entropy. The uncertainty in entropy due to the experimental contributions are limited to within 10%.

C. Measurement of resistivity in steady and pulsed magnetic fields

We measured the resistivity using a standard four probe method. For making the contacts, four gold contact pads were evaporated on the sample and the contacts to the sample were subsequently made by soldering $40 \mu\text{m}$ copper wires using Ag—In solder. Most of the MR data were taken by a superconducting solenoid producing steady field up to 12 T. For comparison, we have also used a pulsed magnet to make the resistivity measurements. The pulsed field with $\mu_0 H_{peak} = 14$ T has a fall time 20 msec. The data acquisition was done with a 12 bit 20 MHz card. In case of the superconducting magnet the data were taken by fixing the field and varying the temperature. In case of the pulsed magnet it was field scans at fixed temperatures. Since we are in a regime where there is no noticeable hysteresis effects both the methods should lead to the same result provided the field and temperature calibration has the same traceability. We find

that the data taken by the steady field and the pulsed field are close within experimental uncertainty. In the results presented we do not distinguish the data taken by the two methods and present them together.

III. RESULTS

The results are presented in three subsections. In the first subsection, we discuss the specific heat as a function of temperature at different magnetic fields. The second subsection contains results of the entropy changes at the CO transition at different fields. Finally, we present the results obtained from resistance measurements at different fields and temperatures.

A. Specific heat as a function of temperature and magnetic field

A waterfall plot of specific heat as a function of temperature at different magnetic fields is shown in Fig. 2 (The data are offset for clarity). In zero field, the sample shows a first order CO transition at $T_{CO} = 235$ K and a small step at ≈ 165 K which is the Néel temperature T_N . The zero field specific heat data are shown as inset in Fig. 2 for an extended

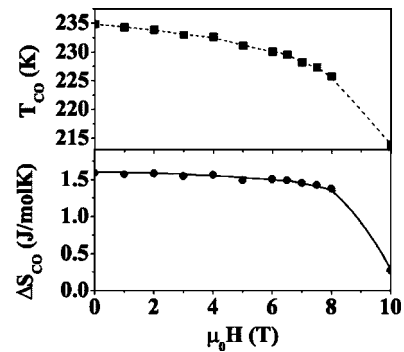


FIG. 3. (a) T_{CO} as a function of applied magnetic field. (b) Change in entropy at the CO transition as a function of field.

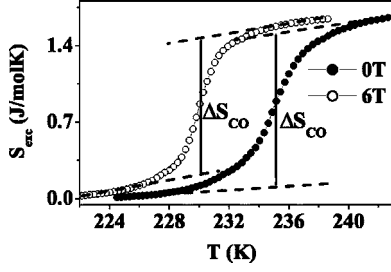


FIG. 4. S_{exc} as a function of temperature for fields of 0 T and 6 T.

temperature scale. In the specific heat data with increasing magnetic field, the T_{CO} shifts to lower temperatures. A plot of T_{CO} as a function of the field is shown in Fig. 3. We see that a field of 10 T shifts the T_{CO} by as much as 20 K. It can be seen from Fig. 3 that there are two regions. For $\mu_0 H < 6$ T, the change in T_{CO} is gradual while for $\mu_0 H > 6$ T, it is rather rapid. Close to 10 T we see the transition as just a sharp line and essentially no width as limited by the experimental setup. We show below that with increasing field, we ultimately reach a point where the entropy change at T_{CO} vanishes.

B. Entropy change at T_{CO}

It has been established by calorimetric investigations that there is a change in entropy ΔS_{CO} at the charge ordering transition. In zero field, $\Delta S_{CO} \approx 1.6$ J/mol K.¹³ The earlier data were obtained by conventional adiabatic calorimetry wherein the data are taken while heating while the present data were taken by continuous cooling calorimetry wherein the data are taken during cooling. Comparing the peak height or width taken by these two completely different methods may be difficult as there is an inherent error present in determining the peak width in first order transitions. What can

be compared is the entropy change at the transition ΔS_{CO} as this is the area under the peak in specific heat divided by the temperature. This ΔS_{CO} for both data match to within experimental uncertainties. For calculating the entropy change during the CO transition, a background lattice contribution has to be first subtracted out from the specific heat data. We define $C_{exc} = C - C_{lattice}$. For estimation of $C_{lattice}$ we employ the procedure described in detail in Ref. 13. The entropy change is calculated by numerically integrating C_{exc}/T as $S_{exc} = \int_{200}^T (C_{exc}/T) dT$. The lower limit of integration (200 K) is so chosen that $C_{exc} \approx 0$ for all $\mu_0 H$ at this temperature. Figure 4 shows the S_{exc} as a function of temperature near T_{CO} . To obtain the change in entropy ΔS_{CO} at the transition we linearly extrapolate the values of S_{exc} above and below the transition and find the difference in the extrapolated values at the transition. By this procedure we obtain a ΔS_{CO} of ≈ 1.6 J/mol K at 0 T. (Note that this procedure does introduce uncertainty in the absolute value of ΔS_{CO} which we estimate $\approx 10\%$).

A plot of the calculated ΔS_{CO} as a function of field is shown in Fig. 3. The decrease in ΔS_{CO} is small up to a field of 6 T. Above this, the fall is very rapid. The important fact that we have established is that $\Delta S_{CO} \rightarrow 0$ as the field is increased. From our calorimetry data, we could clearly identify the point B as $T^* \approx 215$ K, $\mu_0 H^* \approx 10.5$ T where $\Delta S_{CO} \approx 0$. Our transport measurements showed that at $\mu_0 H^*$ the CO transition ceases to exist.

As pointed out earlier, no marked signature except a small feature is observable at low T as we cross the line CB. This becomes weaker as $\mu_0 H$ increases. Thus vanishing of ΔS_{CO} as we move along the line AB is compatible with the fact that the two lines of transition meet at the point B where $\Delta S_{CO} \approx 0$. We point out that vanishing of the entropy ΔS_{CO} at a certain field is a new observation and we explain below that it is linked to the stability of the CO state.

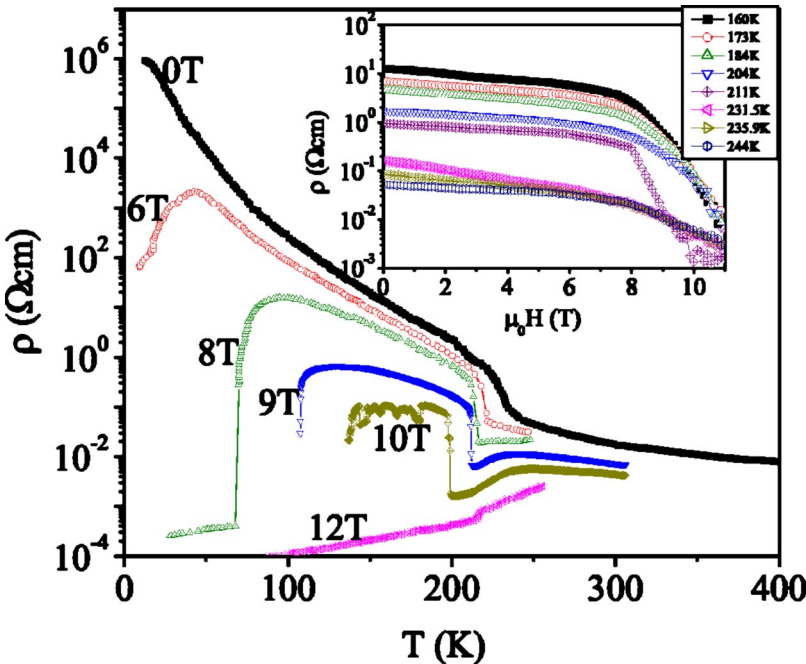


FIG. 5. Resistivity as a function of temperature for a few representative fields. Inset shows resistivity as a function of field at different temperatures.

($260\text{ K} > T > T_{CO}$) is therefore an interesting phenomenon.

The insulating phase above T_{CO} , like other colossal magnetoresistive (CMR) systems, is attributed to Jahn-Teller (JT) distortion. In the undoped parent compound such as PrMnO_3 or LaMnO_3 , the high-temperature JT distortion can be cooperative in nature leading to orbital ordering. This leads to an insulating state in these samples. Hole-doping (by substitution of a bivalent cation in the rare-earth site) leads to a dilution of the cooperative JT and orbital ordering although the high-temperature insulating phase is retained. Past studies (using resonant x-ray scattering technique or neutron scattering technique¹⁶) have shown some degree of orbital or charge order above T_{CO} , albeit with a small correlation length. The suppression of the insulating phase at $T > T_{CO}$ would mean that a high enough magnetic field can suppress this local ordering leading to a metallic state with $d\rho/dT > 0$, although in a limited temperature range. An interesting possibility is that the magnetic field increases the width of the conduction band and thus suppresses polaronic effects and local orbital ordering. It is possible to model the behavior as coexistence of two phases: (both paramagnetic) one metallic and the other insulating. The application of a magnetic field increases the volume fraction of the metallic phase. The increase in volume fraction beyond a certain value leads to crossover to the metallic state. However, at high enough temperature the degree of spin ordering even at high field may not be large enough to cause any effect on the polaronic or local orbital ordering thus stabilizing the insulating state. The metallic and insulating phases are identified as a change in $d\rho/dT$, that occurs when the magnetic field reduces the resistivity to about $20\text{ m}\Omega\text{ cm}$. Interestingly, this is the range of ρ where a metal-insulator transition occurs in many perovskite oxides.¹⁷

The issue of magnetic transition at high fields (transition from the metallic to ferromagnetic metallic phase) is not very clear at this stage in the absence of high field magnetization data. We note that even at a field of 10 T in the vicinity of 250 K the ratio B/T is not large enough to produce substantial spin alignment. (We are dealing with a $S=3/2$ system which is the core t_{2g} spin.) As a result the metallic phase that arises from the PI is likely to be paramagnetic. At low temperatures in a magnetic field the ground state is a ferromagnetic metallic phase. There appears to be some kind of transition or crossover as can be seen from the resistivity data at 12 T in the vicinity of 215 K . This being a transition in a magnetic field can be classified as a field induced ferromagnetic state. To sum up, we propose the scenario that in the vicinity of the phase diagram around the point (H^*, T^*) and at higher temperatures, the magnetic field increases the bandwidth and this suppresses the polaronic nature of the transport and any local charge or orbital order. This lowers T_{CO} and at high enough field no charge or orbital order forms leading to a metallic phase. At still higher field there is field induced ferromagnetic state as the sample is cooled.

In conclusion, using calorimetric and transport investigations, we have shown that beyond a certain magnetic field, the COI state becomes unstable at all T . The stability of the COI state is ensured by a finite ΔS_{CO} . When $\Delta S_{CO} \rightarrow 0$, on the application of a magnetic field the COI state becomes unstable.

ACKNOWLEDGMENTS

A.K.R. acknowledges financial support from DST (Government of India) for a sponsored project and K.S.N. acknowledges CSIR for support.

*Electronic address: ksnaga@physics.iisc.ernet.in

†Electronic address: arup@physics.iisc.ernet.in

¹ *Colossal Magnetoresistance, Charge Ordering and Related Properties of Manganese Oxides*, edited by C. N. R. Rao and B. Raveau (World Scientific, Singapore, 1998).

² *Colossal Magnetoresistive Oxides*, edited by Y. Tokura (Gordon and Breach Science, New York, 2000).

³ A. Asamitsu, Y. Tomioka, H. Kuwahara, and Y. Tokura, *Nature (London)* **388**, 50 (1997).

⁴ K. Ogawa, W. Wei, K. Miyano, Y. Tomioka, and Y. Tokura, *Phys. Rev. B* **57**, R15 033 (1998).

⁵ M. Fiebig, K. Miyano, Y. Tomiyoka, and Y. Tokura, *Science* **280**, 1925 (1998).

⁶ V. Kiryukhin, D. Casa, J. P. Hill, B. Keimer, A. Vigliante, Y. Tomiyoka, and Y. Tokura, *Nature (London)* **386**, 813 (1997).

⁷ Y. Tomioka, A. Asamitsu, H. Kuwahara, Y. Moritomo, and Y. Tokura, *Phys. Rev. B* **53**, R1689 (1996).

⁸ Ayan Guha, A. K. Raychaudhuri, A. R. Raju, and C. N. R. Rao, *Phys. Rev. B* **62**, 5320 (2000).

⁹ J. M. De Teresa, M. R. Ibarra, C. Marquina, P. A. Algarabel, and S. Oseroff, *Phys. Rev. B* **54**, R12 689 (1996).

¹⁰ V. Hardy, A. Wahl, C. Martin, and Ch. Simon, *Phys. Rev. B* **63**,

224403 (2001).

¹¹ V. N. Smolyaninova, K. Ghosh, and R. L. Greene, *Phys. Rev. B* **58**, R14 725 (1998).

¹² A. Anane, J. -P. Renard, L. Reversat, C. Dupas, P. Veillet, M. Viret, L. Pinsard, and A. Revcolevschi, *Phys. Rev. B* **59**, 77 (1999).

¹³ A. K. Raychaudhuri, Ayan Guha, I. Das, R. Rawat, and C. N. R. Rao, *Phys. Rev. B* **64**, 165111 (2001).

¹⁴ M. Rajeswari, Sheela K. Ramasesha, and A. K. Raychaudhuri, *J. Phys. E* **21**, 1072 (1988).

¹⁵ Note: The COI-FMM transition in polycrystalline $\text{Pr}_{0.8}\text{Na}_{0.2}\text{MnO}_3$ have been investigated (Ref. 18). An application of magnetic field of 14 T suppresses the specific heat associated with T_{CO} . However, the issue of entropy at transition has not been discussed. Also the authors did not find any metallic nature at high field presumably due to the polycrystalline nature of the material.

¹⁶ R. Kajimoto, T. Kakeshita, Y. Oohara, H. Yoshizawa, Y. Tomioka, and Y. Tokura, *Phys. Rev. B* **58**, R11 837 (1998).

¹⁷ A. K. Raychaudhuri, *Adv. Phys.* **44**, 21 (1995).

¹⁸ J. Hejtmanek, Z. Jirak, J. Sebek, A. Strejc, and M. Hervieu, *J. Appl. Phys.* **89**, 7413 (2001).